

Supporting Information for

Oriented attachment interfaces of zeolitic imidazolate framework nanocrystals

Xiaocang Han^a, Rui Su^b, Wenqian Chen^{c,d}, Qi Han^e, Yuan Tian^f, Jiuhui Han^c, Xiaodong Wang^a, Shuangxi Song^a, Kolan Madhav Reddy^{a,c}, Hexiang Deng^e, Pan Liu^{a,c*}, Mingwei Chen^{f*}

^aState Key Laboratory of Metal Matrix Composites, School of Materials Science and Engineering, Shanghai Jiao Tong University, Shanghai, 200240, People's Republic of China;

^bCollege of Materials & Environmental Engineering, Hangzhou Dianzi University, Hangzhou 310018, People's Republic of China;

^cAdvanced Institute for Materials Research, Tohoku University, Sendai 980-8577, Japan;

^dSchool of Environmental and Chemical Engineering, Shanghai University, Shanghai 200444, People's Republic of China;

^eKey Laboratory of Biomedical Polymers-Ministry of Education, College of Chemistry and Molecular Sciences, Wuhan University, Wuhan 430072, People's Republic of China;

^fDepartment of Materials Science and Engineering, Johns Hopkins University, Baltimore, MD 21218, USA.

*Corresponding author.

E-mail: P. L (panliu@sjtu.edu.cn) & M. W. Chen (mwchen@jhu.edu)

This PDF file includes:

Experimental section

Supplementary Figures: Figure S1 to S9

Experimental section

Synthesis of rhombic dodecahedral ZIF-67/8 nanocrystals

Nanocrystalline ZIF-67 was synthesized by a hydrothermal method at room temperature. A solution of $\text{Co}(\text{NO}_3)_2 \cdot 6\text{H}_2\text{O}$ (0.5821g, 2 mmol) in 20 mL of methanol (MeOH) is rapidly poured into a solution of 2-methylimidazole (Hmim) precursors (0.1642g, 2 mmol) in 20 mL of methanol under free settling for 2-3 days. ZIF-8 was also synthesized by a solvothermal method at room temperature¹. A solution of $\text{Zn}(\text{NO}_3)_2 \cdot 6\text{H}_2\text{O}$ (0.369 g, 1.24 mmol) in 25 mL of methanol (MeOH) is rapidly poured into a solution of 2-methylimidazole (Hmim) precursors (0.821g, 10 mmol) in 25 mL of methanol under stirring for one hour. The as-synthesized ZIF-67 and ZIF-8 nanocrystals were separated from the milky dispersions by centrifugation and following by repeated washing with fresh methanol for three times. Then, the samples were dried at room temperature under a reduced pressure by mechanical pumping. The dried samples were dispersed in methanol by sonication about 3~5 minutes. After standing still for 3 minutes, the supernatant liquid was dropped onto ultrathin Si_3N_4 membrane (~5 nm) with a silicon-based grid for TEM characterization.

Structure characterization

All HRTEM images were captured by using JEM ARM-200F electron microscope equipped with a spherical aberration corrector (CEOS GmbH) for the image-forming (objective) lens system at 200kV. A direct-detection electron-counting camera (Gatan K2 summit) was employed for the low-dose Cs-corrected HETRM observations ($\text{Cs} \sim 5\mu\text{m}$) in electron-counting mode with Dose-fractionation function. During the TEM image acquisition, we viewed the specimen in diffraction mode to avoid structural damage during sample searching and present enough contrast at a dose rate lower than $\sim 1 \text{ e}^-/\text{\AA}^2/\text{s}$. The HRTEM images were acquired as a collection of frames at a high frame rate instead of a single image with long exposure, which is able to minimize the influence of sample drift on spatial resolution after sample motion correction of subframes.

HRTEM image processing and simulation

A modified low-dose HRTEM image alignment method used for the refined correction of drift have been presented in ref². The drift-corrected HRTEM images were denoised by real-space averaging and Wiener filter which are commonly used in HRTEM to enhance signal-to-noise ratio for extracting crystallographic information from the images. The HRTEM images were simulated by using the commercial *QSTEM* software³. Appropriate imaging parameters and aberration coefficients according to experimental conditions were selected for HRTEM images simulation after setting up the ZIF-67 structure model. Specifically, an accelerating voltage of 200 kV was used, with a spherical aberration of $\sim 1\mu\text{m}$, focal spread of 3 nm, and pixel size of 0.75 Å. The simulated images are calculated using 200 nm defocus value and 30 nm sample thickness.

Strain analysis based on the geometric phase analysis (GPA) method⁴ was performed using the FRWRtools plugin for DigitalMicrograph. The method is based upon centering a small aperture around a strong reflection in the Fourier transform of an HRTEM lattice image and performing an inverse Fourier transform. The phase component of the resulting complex image is shown to give information about local displacements of atomic

planes and the two-dimensional displacement field can be derived by applying the method to two non-colinear Fourier components. Local strain components can be found by analyzing the derivative of the displacement field.

Theoretical calculations of ZIF-8 surface energy

Due to the lack of Co parameters in the “3ob” set, the ZIF-8 was used instead. we expect negligible effect on the final results as interface energies are mostly dominated by hydrogen or vdW interactions between the organic part of ZIFs. In this work, the zigzag-to-zigzag {110} interface energies of ZIF-8 crystals were calculated by Equation 1:

$$E_{AB} = \frac{E_A - E_B}{A}$$

(1)

where E_A and E_B are the energies of the optimized zigzag surface slabs, and A is the surface area of the slab. The {110} surfaces with solvation-correction are assumed to be passivated by species from solvents. The structure relaxation was performed with a force tolerance of 0.04 eV/Å.

Due to a large number of atoms in the ZIF-8 interface cell, the surface energies of modified ZIF-8 surfaces were calculated by a semi-empirical approach within the self-charge-consistent density functional tight-binding (SCC-DFTB) framework as implemented in the DFTB+ code. The optimized cell parameter was determined to be 17.035 Å, and this relaxed cell was used to generate {110} surface models. As the DFTB method uses orbital overlap integrals and repulse potentials parameterized from the DFT data, the description of structure and energetic properties would suffer from the approximating models and DFT dataset used for parameterization. Currently, there are two sets of DFTB parameterizations for the Zinc-organic systems: the Zinc-organic (“Znorg”) parameter set⁵ that was fitted against Zinc contained bulk compounds; and for Zn-organic complexes, the third-order parametrization for organic and biological systems (“3ob”) parameter set⁶ was fitted using the third order density functional tight binding (DFTB3) model. The “3ob” parameterization has been shown to reduce the over-binding errors of organic molecules in the previous “Znorg” parameter set and improve the description of hydrogen bonds⁶. In this work, we choose to use the “3ob” parameterization as it provides better description of lattice constants and surface energies in comparison with the “Znorg” parameterization. Additionally, the non-bonding van der Waals interactions were described by the DFT-D3 method⁷ with the Beck-Johnson damping⁸.

Supplementary Figures

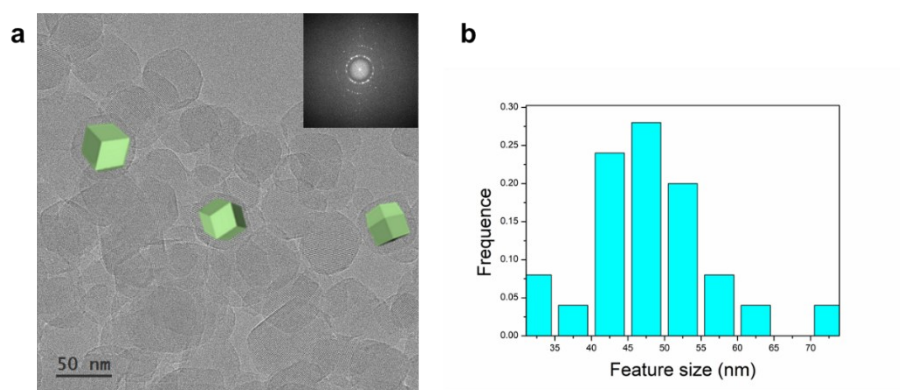


Fig. S1 Morphology and crystals size distribution of ZIF-67. a) Low magnification TEM image displays single crystal and agglomerated nanoparticles. The insertions show the corresponding FFT pattern and projected rhombic dodecahedra models with the same orientation of underneath imaged crystallites. b) Statistical character of ZIF-67 nanocrystals with a size range between 40-60 nm.

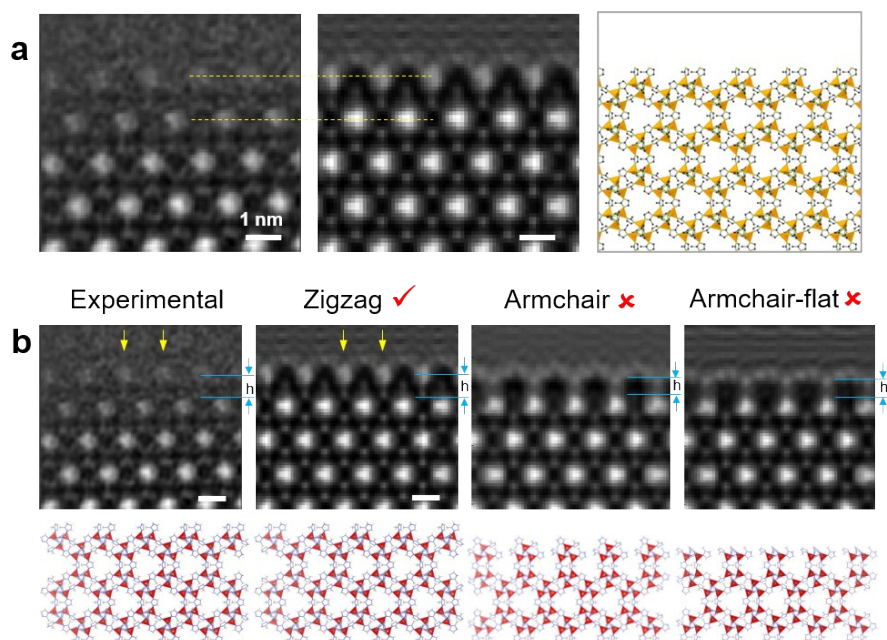


Fig. S2 Zigzag surface termination of a ZIF-67 nanocrystal. a) Experimental, simulated and projected structural model images of ZIF-67 {110} surfaces viewed along the [111] axis. b) The comparison of simulated images based on low-panel surface termination models with real-spacing filtered experimental image along [111] direction at a defocus value of 230nm. Clearly, the surface termination of ZIF-67 is zigzag type. Scale bar, 1nm.

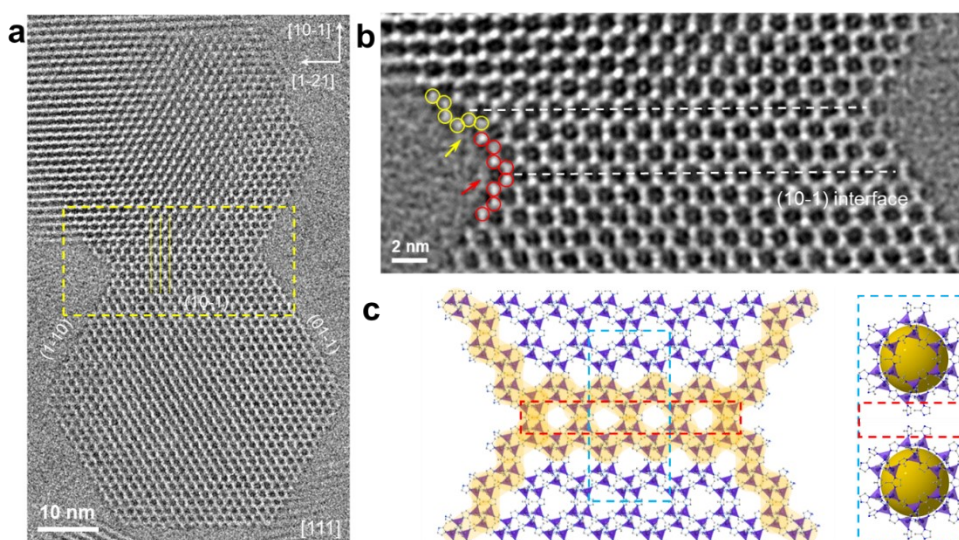


Fig. S3 Coherent {110} interface structures of two-assembled ZIF-8 crystals. **a)** Coherent and perfect {110} interface between two assembled ZIF-8 crystals. This low-dose Cs-corrected HRTEM image of two oriented attached ZIF-8 crystals is taken along [111] axis. The (10-1) lattice plane matches perfectly across the interface after assembly. Yellow lines are used to show the perfect coherence between (-12-1) lattice planes in the two crystals. **b)** An enlarged and denoised HRTEM image extracted from yellow dashed frame in (a). The interface (10-1) is located at white dashed lines. Yellow and red circles highlight Zn triplets. The Yellow arrow show step-edge sites on the zigzag surfaces. Corner sites on interface is denoted by red arrows. **c)** Left, the atomic interfacial structure with regard to two self-assembled crystals viewed along [111] direction showing the perfect arrangement of molecular species as they do in internal structure. Two attached surface plane are linked by a single line of mim ligands denoted by red dashed frame, implying that the absence of a layer of mim ligands in the interface. Right, non-chemical bonding between two approaching cages, indicating that chemical bonding is not involved in perfect interface which shares a single layer of ligands.

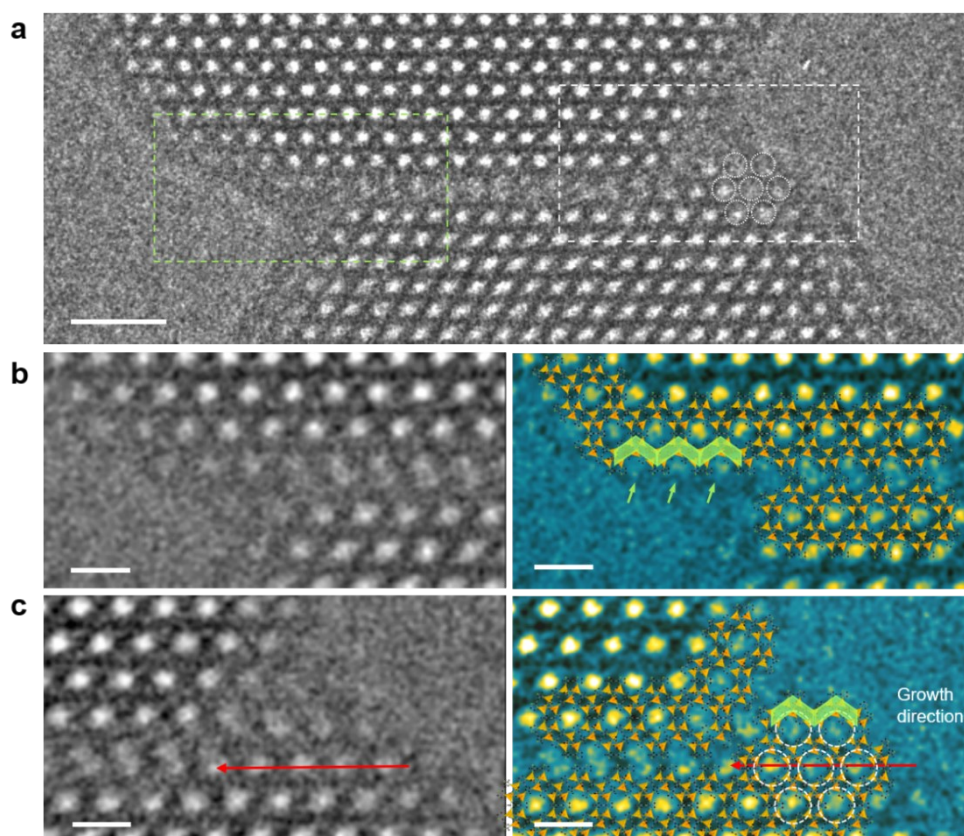


Fig. S4 Zigzag free surface termination of attached ZIF-67 nanocrystals. a) The raw data of Fig. 3a. b) Wiener-filtered HRTEM and colored images (with projected surface cages model inserted) of green box interface region in (a). c) Wiener-filtered HRTEM and colored images (with projected cages model inset) of white box interface region in (a). Clearly, the free surface termination of ZIF-67 is zigzag type. Scale bars in (a, b-c) are 5 nm and 2 nm.

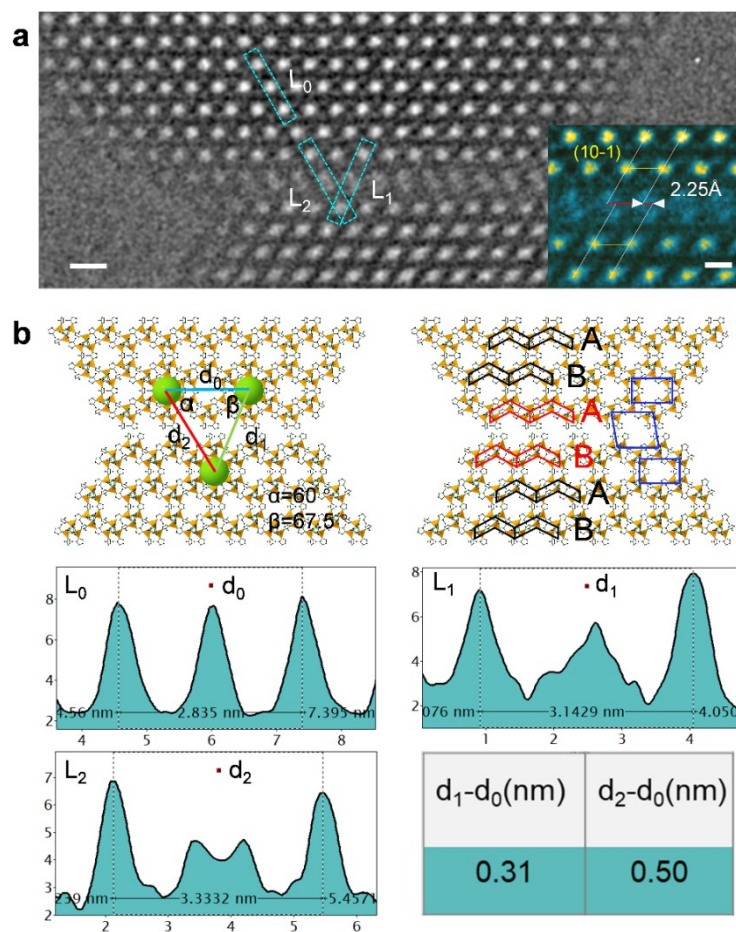


Fig. S5 Separated interface with a spacer layer. **a)** Wiener-filtered HRTEM image of two oriented attached ZIF-67 crystals inserted with a zoom-in and real-spacing superimposing filtered image (4 image motifs). **b)** Identified projected sodalite cages model of zigzag-to-zigzag {110} interfacial structure derived from experimental image in (a) and its stacking sequence. Blue rhomboid represents the shearing of the rectangle units in individual crystals. The intensity profiles drew from corresponding cyan boxes shown in (a). The distance between neighbouring projected sodalite cages belonging to two crystals is labelled d_1 and d_2 , and d_0 refers to standard distance between cages in bulk. The base angles of the triangle formed by three neighbouring projected sodalite cages are labelled α and β as illustrated in projected model image, and the angular difference between α and β is 7.5° . The d_1 and d_2 values at the interfacial region deviated greatly from that in the bulk structure ($d_0=2.835\pm 0.075\text{nm}$, considering the fact that the accuracy of the measurement in HRTEM image is highly determined by the pixel size $\sim 0.075\text{nm}$). The corresponding displacement along the (1-10) and (01-1) corresponding to L1 and L2 lattice plane relative to the bulk lattice is 0.31 nm and 0.5 nm. The stacking displacement along (10-1) interface plane is 2.25 Å shown in upright of (a). Scale bars in (a) are 2 nm and 1 nm.

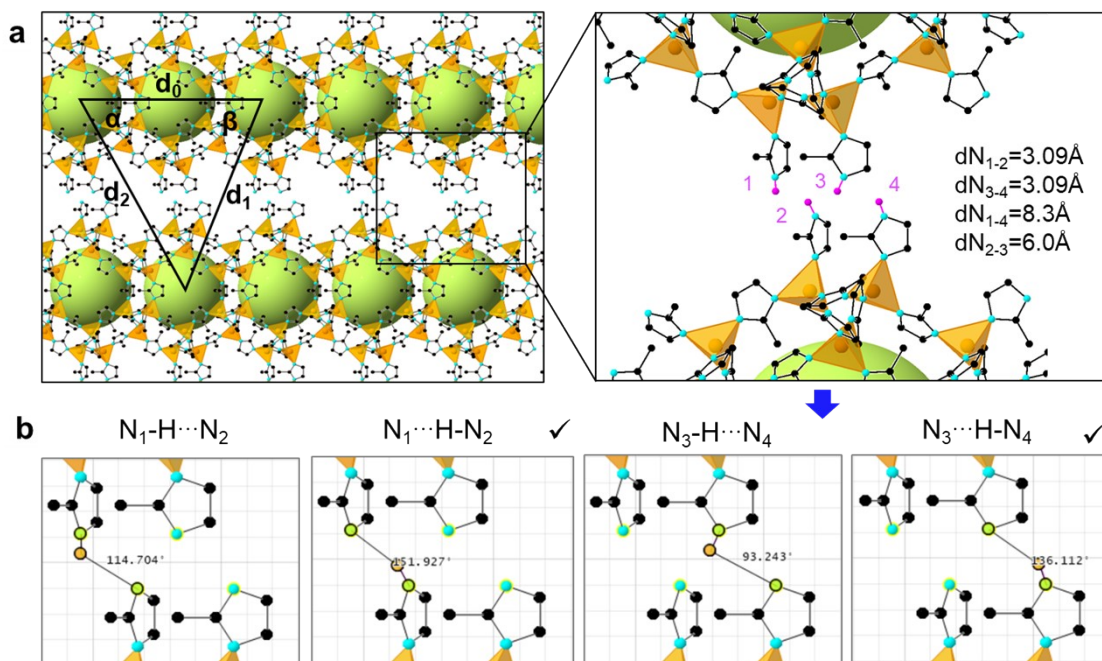


Fig. S6 a) Model geometry of the zigzag-to-zigzag (10-1) interfacial structure formed by two oriented attached ZIF-67 crystal slabs corresponding to the experimental observation. Right panel shows an enlarged view of the interface where multiple hydrogen atoms likely located between the two crystals. The two visually close nitrogen atoms with relative longer distance were excluded from possible formation of hydrogen bonding, such as N_1-N_4 and N_2-N_3 . **b)** The below panel shows an enlarged view of the interface where multiple $mim \cdots Hmim$ hydrogen bonds are likely formed between the N_1-N_2 and N_3-N_4 . The bonding angles and lengths conforming to experience value of hydrogen bonds were selected to be $N_1 \text{---} H \text{---} N_2$ and $N_3 \text{---} H \text{---} N_4$. Cages model: green spheres represent void pore space, cyan and rose red represent N and H atoms, respectively.

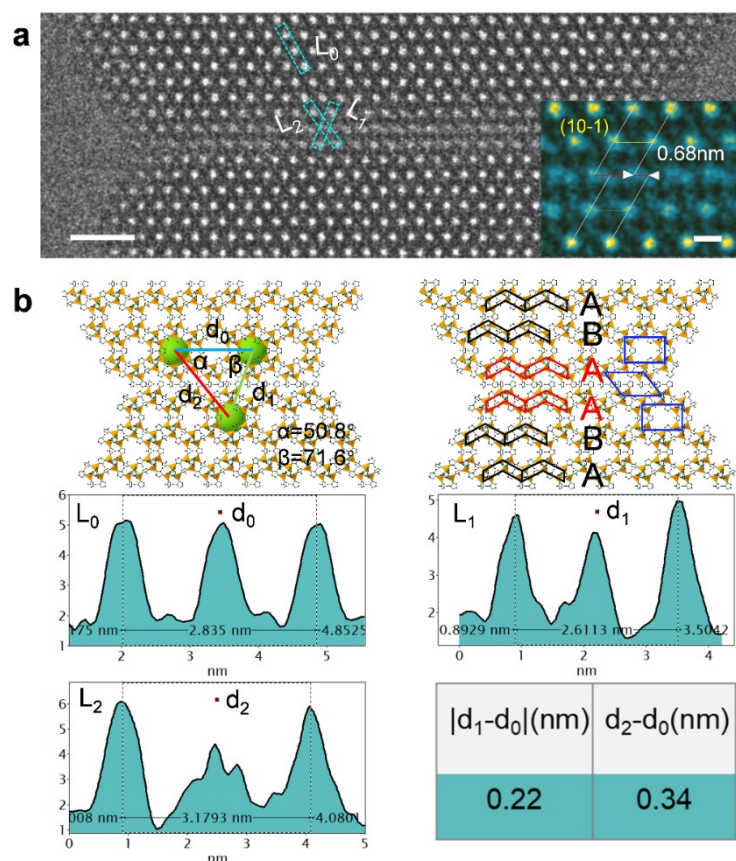


Fig. S7 Incoherent interface with a stacking fault. **a)** Raw HRTEM image of two oriented attached ZIF-67 crystals inserted with a zoom-in and real-spacing superimposing filtered image (6 image motifs). **b)** Identified projected sodalite cages model of zigzag-to-zigzag $\{110\}$ interfacial structure derived from experimental image in **(a)** and its stacking sequence. Blue rhomboid represents the shearing of the rectangle units in individual crystals. The intensity profiles drawn from corresponding cyan boxes shown in **(a)**. The distance between neighbouring projected sodalite cages belonging to two crystals is labelled d_1 and d_2 , and d_0 refers to standard distance between cages in bulk. The base angles of the triangle formed by three neighbouring projected sodalite cages are labelled α and β as illustrated in projected model image, and the angular difference between α and β is 20.8° . The d_1 and d_2 values at the interfacial region deviated greatly from that in the bulk structure ($d_0=2.835\pm 0.075$ nm). The corresponding displacement along the (1-10) and (01-1) lattice plane (marked by L1 and L2 lines) relative to the crystal lattice is 0.22 nm and 0.34 nm. The stacking displacement along (10-1) interface plane is 0.68 ± 0.075 nm shown in upright of **(a)**. Scale bars in **(a)** are 5 nm and 1 nm, respectively.

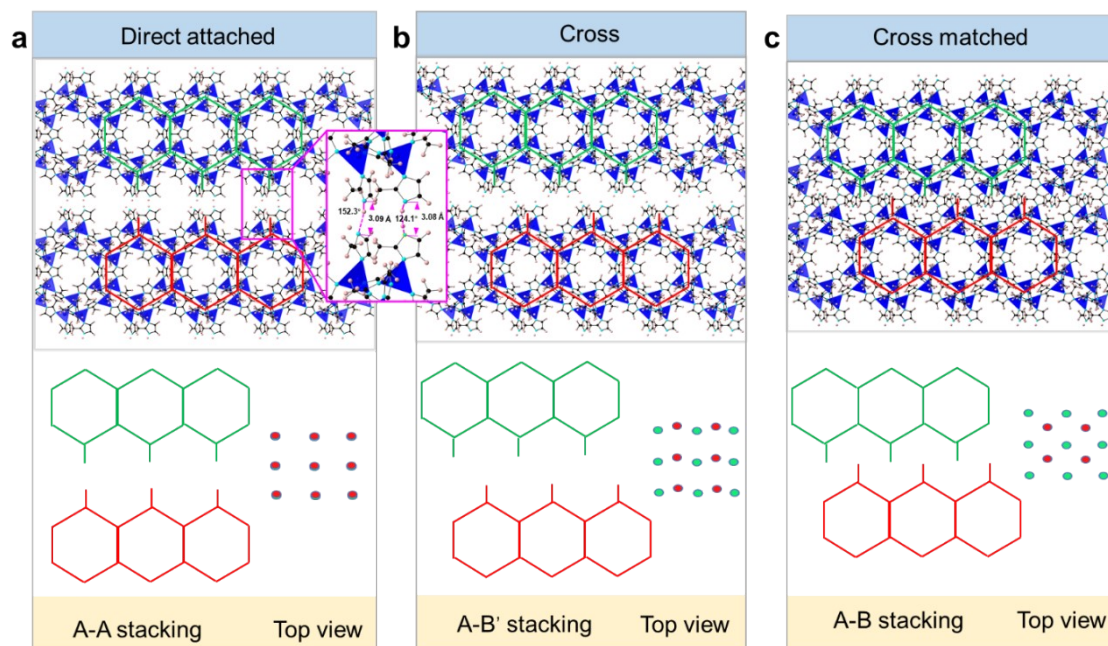


Fig. S8 Optimized geometry of the zigzag-to-zigzag (110) interface structure models formed by two oriented attached ZIF-8 crystal slabs using SCC-DFTB methods. **a-c)** The direct attached, cross, and cross matched OA interface structures. The below panel shows the cages stacking from front view and top view. The cages were marked by colored hexagons and solid circles. Here all under-coordinated Zn sites are capped by Hmim ligands. Inset in (a) shows an enlarged view of the interface where multiple $\text{mim} \cdots \text{Hmim}$ hydrogen bonds are formed between the two direct attached crystal slabs, while no hydrogen bonds formed in (b) and (c).

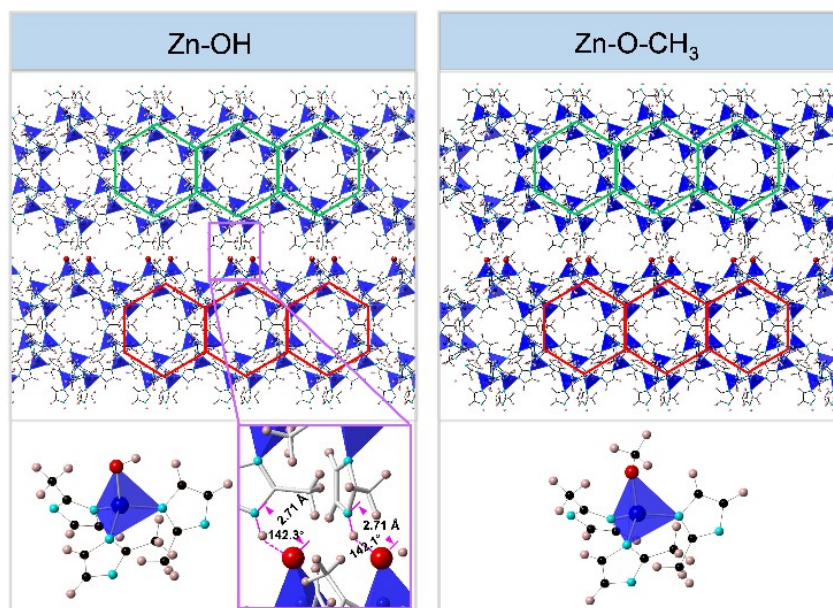


Fig. S9 The optimized zigzag-to-zigzag interface structure models of ZIF-8 with under-coordinated Zn sites capped by the mixture of Hmim and water or methanol.

References

- 1 J. Cravillon, S. Münzer, S. J. Lohmeier, A. Feldhoff, K. Huber and M. Wiebcke, *Chem. Mater.*, 2009, **21**, 1410–1412.
- 2 X. Han, P. Liu, F. Lin, W. Chen, R. Luo, Q. Han, Z. Jiang, X. Wang, S. Song, K. M. Reddy, H. Deng and M. Chen, *Angew. Chem. Int. Ed.*, 2020, **59**, 21419–21424.
- 3 C. Koch, *Dissertation*.
- 4 M. J. Hÿtch, E. Snoeck and R. Kilaas, *Ultramicroscopy*, 1998, **74**, 131–146.
- 5 N. H. Moreira, G. Dolgonos, B. Aradi, A. L. Da Rosa and T. Frauenheim, *J. Chem. Theory Comput.*, 2009, **5**, 605–614.
- 6 X. Lu, M. Gaus, M. Elstner and Q. Cui, *J. Phys. Chem. B*, 2015, **119**, 1062–1082.
- 7 S. Grimme, J. Antony, S. Ehrlich and H. Krieg, *J. Chem. Phys.*, 2010, **132**, 154104.
- 8 S. Grimme, S. Ehrlich and Lars Goerigk, *J. Comput. Chem.*, 2011, **32**, 1456–1465.